

---

# A codimension-four singularity with potential for action

BERND KRAUSKOPF and HINKE M. OSINGA

Department of Mathematics, The University of Auckland, New Zealand.

**Summary.** We review how a conjectural codimension-four unfolding of the full family of cubic Liénard equations helped to identify the central singularity as an excellent candidate for the organizing center that unifies different types of spiking action potentials of excitable cells. This point of view and the subsequent numerical investigation of the respective bifurcation diagrams led, in turn, to new insight on how this codimension-four unfolding manifests itself as a sequence of bifurcation diagrams on the surface of a sphere.

In 1952, Hodgkin and Huxley [10] formulated the first realistic mathematical model describing the flow of electric current through the surface membrane of a squid giant axon. Their system produces a sequence of single action potentials, which are equivalent to the relaxation oscillations generated by a simple RCL-circuit (involving a resistor, capacitor and inductor) such as the Van der Pol oscillator [16, 17]. Electrically excitable cells can exhibit many other bursting patterns, which can loosely be interpreted as a series of spikes (action potentials) modulated by a slower relaxation oscillation. The bursting is related to and controlled by ionic currents through channels in the cell wall, which evolve on much slower time scales. Rinzel [18, 19] was the first to explain such bursting patterns mathematically in terms of an underlying bifurcation diagram with a hysteresis loop, which is traversed by one or more slowly varying parameters; see also [11].

The bursting pattern one finds depends on the codimension-one bifurcations that are encountered, that is, on the relative positions of saddle-node bifurcations, Hopf bifurcations and homoclinic bifurcations that are crossed by the slowly varying parameter. These occur naturally near codimension-two Bogdanov–Takens bifurcations in two-parameter bifurcation diagrams of planar systems which, therefore, arise as ‘minimal models’ of bursting patterns of action potentials. The classification of bursting patterns was formalized further by studying the transitions between them via parameter dependence of the underlying bifurcation diagram. In particular, the organisation of the two-parameter bifurcation diagram under consideration changes when the Bogdanov–Takens bifurcation itself undergoes a bifurcation, which is an event of codimension three where a higher-order normal-form term vanishes. This realization is behind the work of Bertram, Butte, Kiemel and Sherman [2], who presented many known bursting patterns as generated by horizontal parameter paths through a two-parameter bifurcation diagram of the Chay–Cook model, which is a

paradigm model that retains many physiological features and is representative for a large class of realistic models of neuronal spiking. They realized that this bifurcation diagram of the Chay–Cook model can be found as a slice in the three-parameter unfolding of the degenerate Bogdanov–Takens singularity of focus type (or nilpotent cusp of order three) — one of the classic codimension-three bifurcations, with a two-dimensional center manifold, whose unfolding in planar vector fields was presented in [6]; see already case (M) of Fig. 1. This point of view was made explicit in the paper by Golubitsky, Josić and Kaper [7], who proposed a classification of bursting patterns in terms of the smallest codimension of a singularity in whose unfolding it can be generated (via a path of one or more slow parameters). In particular, they showed that so-called fold/homoclinic or square-wave bursting, which involves a hysteresis loop generated by a saddle-node and homoclinic bifurcation, requires an underlying codimension-three singularity, such as the degenerate Bogdanov–Takens singularity of focus type considered in [2].

It emerged that one type of bursting, called pseudo-plateau bursting — first analyzed in [20] and also known as fold/subHopf bursting — could not be found in the unfolding of this codimension-three singularity. This was puzzling because, for biological reasons, it was considered to be related to fold/homoclinic bursting, which is part of the patterns found in [2]. Recent work by Osinga, Sherman and Tsaneva-Atanasova [15] showed that all the relevant types of bursting, including fold/subHopf and fold/homoclinic bursting, can be found near a doubly degenerate Bogdanov–Takens singularity, whose conjectural unfolding was presented in 1998 by Khibnik, Krauskopf and Rousseau [12]. As a result, this codimension-four singularity and its unfolding has enjoyed particular interest from mathematical biologists. Quite amazingly, it emerged as a natural organizing center that unifies an entire class of different bursting patterns of electrically excitable cells.

We now proceed in Sec. 1 by recalling the candidate unfolding of the doubly-degenerate Bogdanov–Takens bifurcation from [12] and review in Sec. 2 the results from [15] on the identification of fold/subHopf bursting near this singularity. Section 3 then presents numerical results on the nature of the codimension-four unfolding in terms of bifurcation diagrams on spheres. In particular, we show that all topologically different bifurcation diagrams can be found readily on spheres of appropriate radii; this point of view is particularly helpful for identifying two-parameter sections that feature certain bursting patterns of interest. We summarise and draw some conclusions in Sec. 4.

## 1 Candidate four-parameter unfolding

In the final section of the paper [12] the four-parameter planar vector field

$$\begin{cases} \dot{x} = y, \\ \dot{y} = \mu_1 + \mu_2 x + \mu_3 y + \mu_4 xy - x^3 - x^2 y, \end{cases} \quad (1)$$

was considered. It represents a candidate unfolding that provides a connection between two codimension-three bifurcations: the case  $\mu_4 = 0$ , which was the main subject of study in [12], and the case of sufficiently large  $\mu_4$ , when (1) represents a nilpotent focus of codimension three as studied in [6]. In fact, when the four parameters  $\mu_i$  are allowed to vary over the reals, (1) represents the full family of cubic Liénard equations.

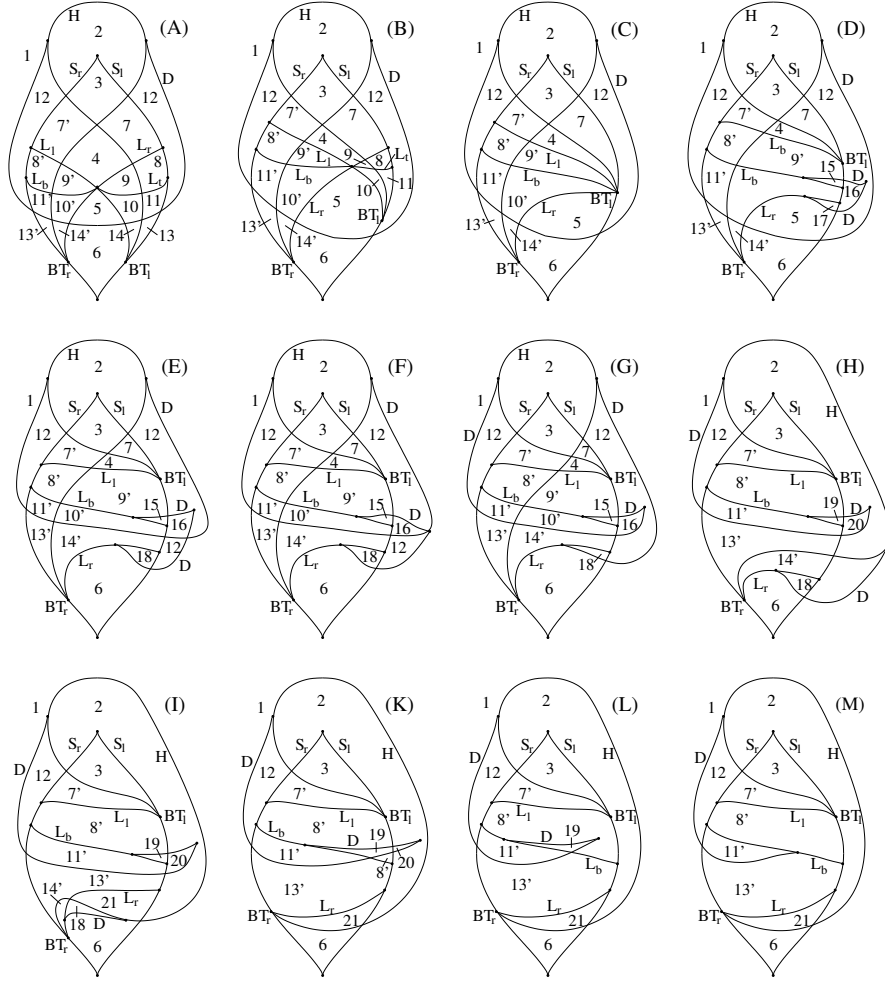


**Fig. 1.** Sketch of the suggested transition with increasing  $\mu_4$  between codimension-three unfoldings on a sphere in  $(\mu_1, \mu_2, \mu_3)$ -space of (1); the associated phase portraits can be found in Fig. 2. Reproduced with permission from [12]. ©1998 IOP Publishing & London Mathematical Society. All rights reserved.

The point of view taken in [12] was to consider the transition of the three-parameter bifurcation diagram of (1) in  $(\mu_1, \mu_2, \mu_3)$ -space as the parameter  $\mu_4$  is varied between these two known cases of  $\mu_4 = 0$  and  $\mu_4$  sufficiently large. The respective three-parameter bifurcation diagram for a given value of  $\mu_4$  can be represented conveniently on the surface of a sphere in  $(\mu_1, \mu_2, \mu_3)$ -space (due to cone structure of the unfolding); it changes qualitatively on the sphere at non-generic values of  $\mu_4$ , which include different types of codimension-three singularities. Importantly, there are quite a number of events of codimension ‘one-plus-two’, where a bifurcation curve moves over a codimension-two bifurcation point on the sphere.

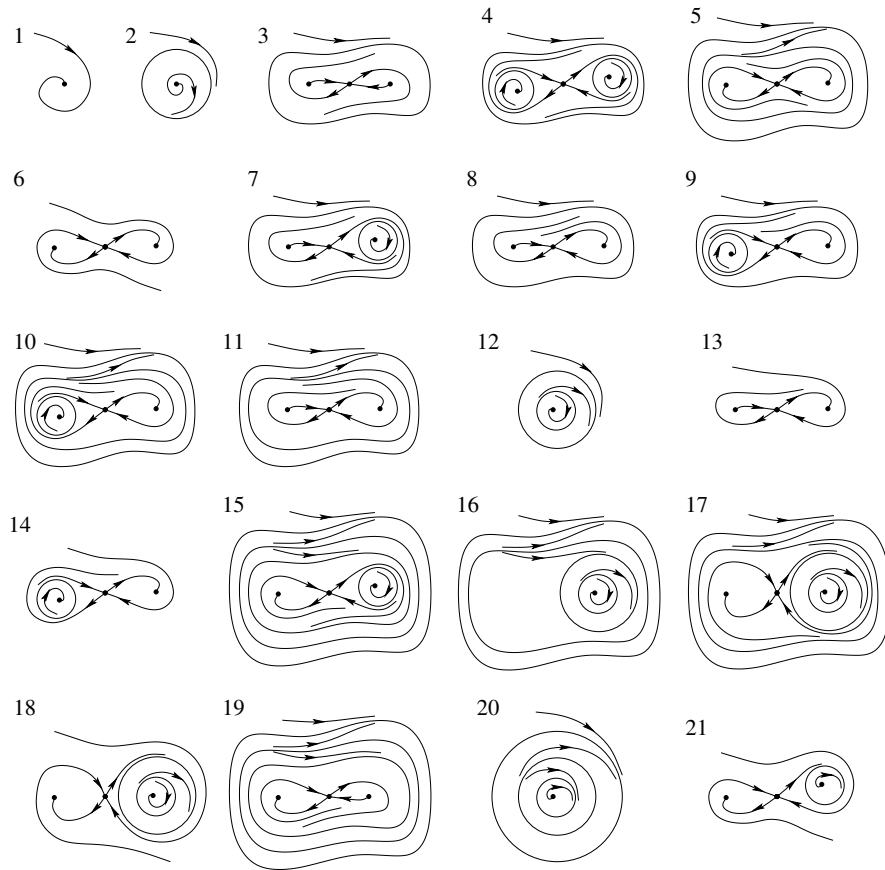


**Fig. 2.** Phase portraits of (1) in the open regions of the bifurcation diagrams in Fig. 1. Reproduced with permission from [12]. ©1998 IOP Publishing & London Mathematical Society. All rights reserved.

Figure 1 reproduces from [12] the respective series of sketched bifurcation diagrams (A) to (M) on the sphere (represented in stereographic projection), and Fig. 2 reproduces the associated phase portraits. The starting point is the reflectionally symmetric bifurcation diagram (A) for  $\mu_4 = 0$ ; details and the proof of correctness can be found in [12]. There is then a first event of codimension ‘one-plus-two’, when the curve D of double (or saddle-node) limit cycles crosses over the Bogdanov–Takens bifurcation point  $BT_l$ , yielding bifurcation diagram (B). At (C) there is a cuspidal loop formed by the separatrices of a Bogdanov–Takens point, which then gives bifurcation diagram (D). The curve D then moves up and at (F) there is a limit cycle of multiplicity four; it is unfolded by a swallow tail yielding (G). In a sequence of events of codimension ‘one-plus-two’ the curve H of Hopf bifurcation them moves past the Bogdanov–Takens bifurcations and beyond to give bifurcation diagram (H), and then the degenerate Hopf point on H moves across the saddle-node bifurcation curve  $S_l$  to result in (I). Then there is a cusp of order three,

yielding (K), after which the cusp point on D moves over  $S_l$  to yield bifurcation diagram (L). Finally, there is a homoclinic loop of order three and the final result is bifurcation diagram (M), which is that of the nilpotent focus; compare with [1, 6].

This sequence of unfoldings (A) to (M) in Fig. 1 takes into account the information available at the time, especially that on different codimension-three bifurcations. The existence of the cuspidal loop had been studied in [22] and, except for the limit cycle of multiplicity four, the stated codimension-three bifurcations had been noted explicitly in [3]; moreover, rigorous numerics in [9, 14] showed the existence of a small region with four limit cycles. The overall unfolding of (1) in Fig. 1 was constructed abstractly in [12] in the spirit of a ‘minimal model’ and it is, hence, conjectural, specifically in terms of the exact sequence of codimension-three and codimension one-plus-two bifurcations.

## 2 Identification of fold/sub-Hopf bursting

Bertram, Butte, Kiemel and Sherman [2] considered a two-parameter slice near the degenerate Bogdanov–Takens singularity of focus type, where the two saddle-node curves are parallel vertical lines. This corresponds to the  $(\mu_1, \mu_3)$ -plane with  $\mu_2 = \text{const} < 0$  and  $\mu_4$  sufficiently large in (1); see case (M) in Fig. 1. The different bursters were identified as different horizontal parameter paths in this parameter plane, along which  $\mu_1$  changes back and forth slowly.

In a similar spirit, Osinga, Sherman and Tsaneva-Atanasova [15] were guided by the bifurcation diagrams in Fig. 1 and presented the fold/subHopf or pseudo-plateau burster by a suitable horizontal path on the relevant bifurcation diagram on the unit sphere in  $(\mu_1, \mu_2, \mu_3)$ -space for  $\mu_4 = 0.75$ . Figure 3 reproduces from [15] the bifurcation diagram and the path on the unit sphere, as well as the time series and phase-space representation of the ensuing fold/subHopf bursting. More specifically, the path is parameterized by  $\mu_1 \in [-0.38, 0.38]$ , with  $\mu_2 = \sqrt{1 - \mu_1^2 - \mu_3^2}$ ,  $\mu_3 = 0.1$  and  $\mu_4 = 0.75$ . System (1) exhibits along this path the saddle-node bifurcation of equilibria  $S_l$ , the homoclinic bifurcation L, the subcritical Hopf bifurcation H, the other saddle-node bifurcation of equilibria  $S_l$ . For consistency of presentation, images from [15] are reproduced here with parameters and notation as used in [12]. In fact, in [15]  $\mu_3 = \nu$ ,  $\mu_4 = b$ , and  $\mu_1$  has the opposite sign; moreover, the curves  $S_l$ ,  $S_r$ , H, D,  $L_l$ ,  $L_b$  and  $L_r$  here are referred to in [15] as  $SN_l$ ,  $SN_r$ ,  $H_l$  or  $H_r$ ,  $SNP$ ,  $HC_l$ ,  $HC_c$  and  $HC_r$ , respectively. The relevant features of the bifurcation diagram on the sphere in Fig. 3(a) correspond qualitatively to a situation in between cases (G) and (H) in Fig. 1; a difference is that (G) and (H) feature a cusp bifurcation point on the curve D of double limit cycles in Fig. 3.

The bursting pattern is generated by introducing a slow variable defined by

$$z(t) = -\mu_1(t) := -0.38 \sin(\varepsilon t),$$

where the time-scale separation parameter  $\varepsilon = 0.1 > 0$  is small (but not so small that delayed bifurcation phenomena are encountered). The  $x$ -coordinate of system (1) represents the membrane potential, and it exhibits the particular bursting pattern known as fold/subHopf or pseudo-plateau bursting [20]; its time series is shown in Fig. 3(b) together with the time series of the slow variable  $z(t) = -\mu_1(t)$ .

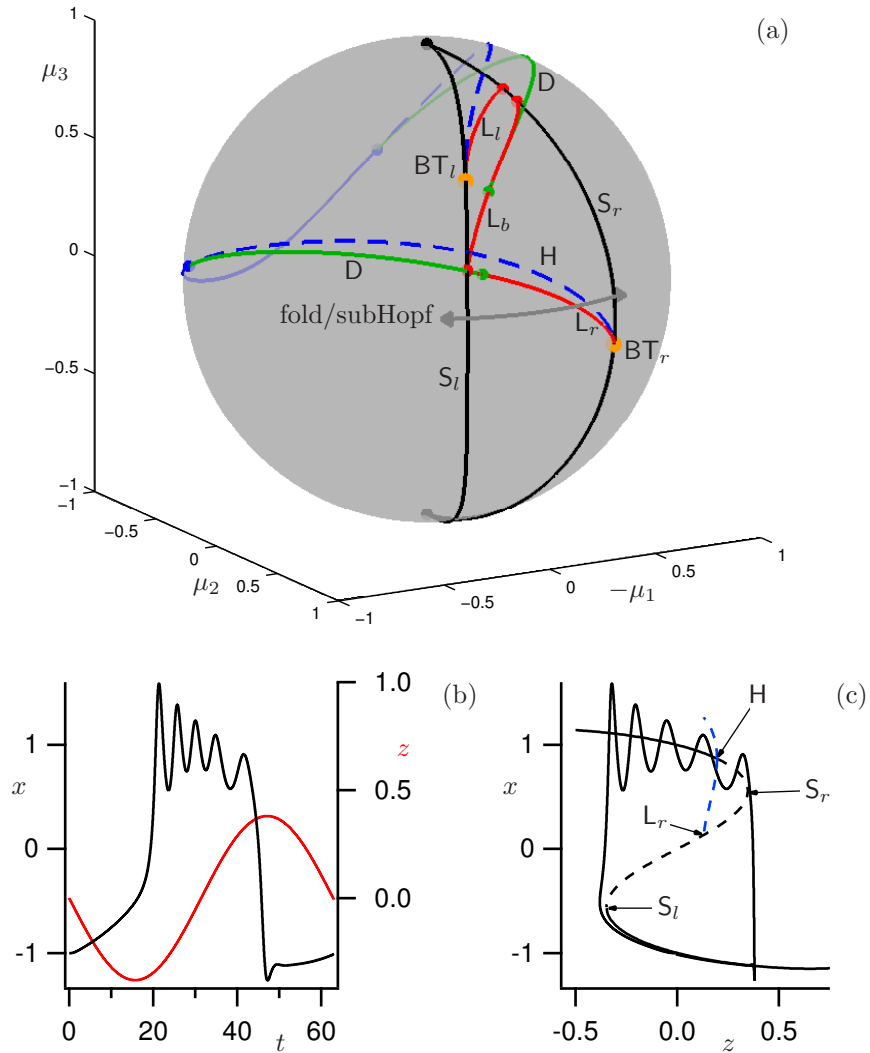


**Fig. 3.** Fold/subHopf bursting for system (1) as generated by a parameter path on the unit sphere in  $(-\mu_1, \mu_2, \mu_3)$ -space with  $\mu_4 = 0.75$ . Panel (a) shows the bifurcation diagram and the path on the unit sphere. Panels (b) and (c) show the time series and the underlying bifurcation diagram of the corresponding fold/subHopf bursting pattern. Reproduced with permission from [15]. ©2012 American Institute of Mathematical Sciences. All rights reserved.

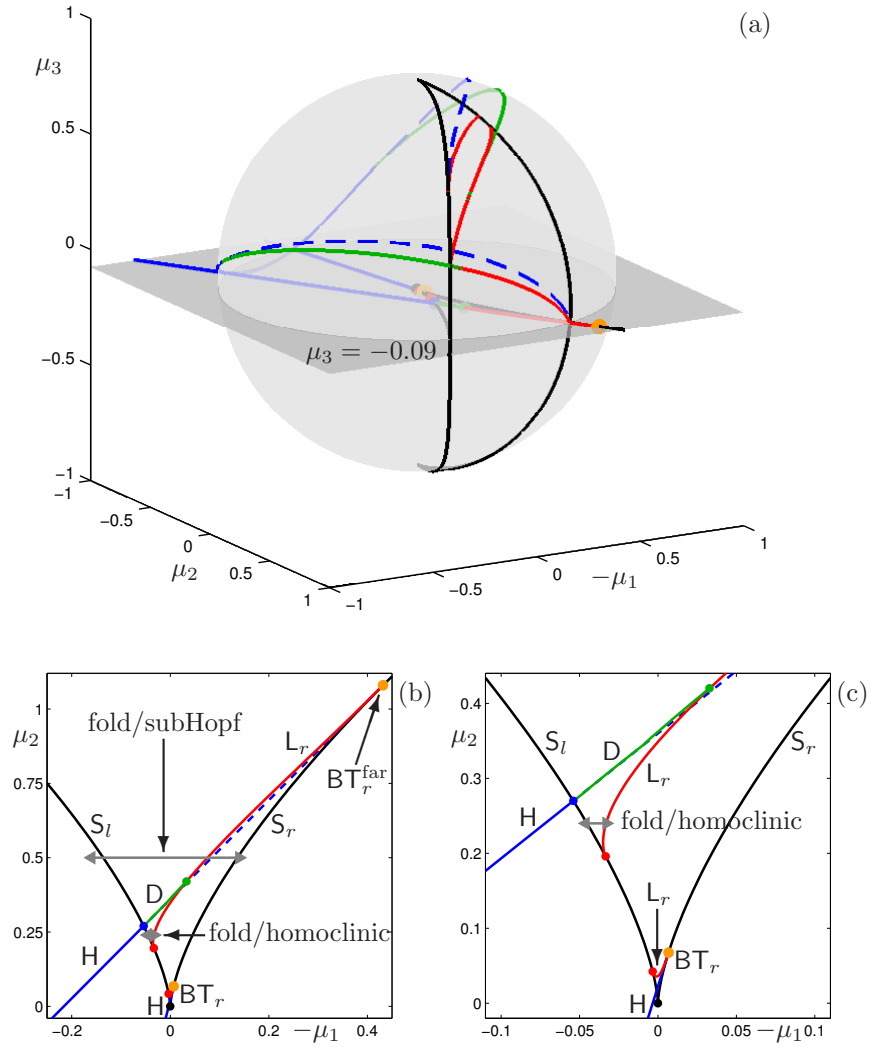


**Fig. 4.** A transition from fold/subHopf to fold/homoclinic bursting for system (1) can be obtained by considering the section  $\mu_3 = -0.09$  for  $\mu_4 = 0.75$ . Panel (a) shows this section relative to the unit sphere, and panel (b) and the enlargement (c) show the bifurcation diagram on this section, together with parameter paths giving rise to fold/subHopf and fold/homoclinic bursting. Reproduced with permission from [15]. ©2012 American Institute of Mathematical Sciences. All rights reserved.

The biologically distinguishing aspects of fold/subHopf bursting are its relatively short period and the small amplitudes of the spikes on the plateau [20]; see also [8, 13, 21]. In contrast to fold/homoclinic or square-wave bursting, the spikes are not stable oscillations but rather transient oscillations that damp down to an upper steady state. Hence, if the time-scale separation parameter is too small, the time series will consist of relaxation oscillations instead. Fold/subHopf bursting only arises if the contraction to the upper steady states is weak relative to the speed of the slow variable.

Figure 3(c) shows the underlying periodic oscillation overlaid onto the bifurcation diagram in the  $(z, x)$ -plane. As can be checked, fold/subHopf bursting cannot be generated by any path on the two-parameter bifurcation diagram in [2].

Indeed, it has been argued in [15] that fold/subHopf or pseudo-plateau bursting can only be generated in the vicinity of a codimension-four singularity, such as that in system (1). However, the bursting patterns of fold/subHopf and fold/homoclinic bursting are considered very similar and it is often hard to distinguish the two types in experiments. Indeed fold/homoclinic or square-wave bursting was found in [2] near the degenerate Bogdanov–Takens singularity of focus type, that is, in system (1) for sufficiently large  $\mu_4$ . Hence, it seems natural to expect the existence of a parameter path in the full four-dimensional parameter space of system (1) that generates fold/homoclinic bursting. Furthermore, it should be possible to deform and/or move this path such that the type of bursting changes to fold/subHopf bursting. In order to find such a transition, the four-dimensional  $(\mu_1, \mu_2, \mu_3, \mu_4)$ -space of system (1) was explored in [15] by setting  $\mu_4 = 0.75$  and considering horizontal or vertical sections chosen appropriately relative to the bifurcation diagram on the sphere. The section for  $\mu_2 = 0.0675$  (not shown; see [15]) gives an associated bifurcation diagram in the  $(\mu_1, \mu_3)$ -plane that is exactly that near the degenerate Bogdanov–Takens singularity of focus type presented in [2].

Furthermore, the choice  $\mu_3 = -0.09$  gives a bifurcation diagram in the  $(-\mu_1, \mu_2)$ -plane that features paths for both fold/subHopf and fold/homoclinic bursting, thus, providing the sought connection between the two. This is illustrated in Fig. 4 reproduced from [15] (with  $-\mu_1$  along the horizontal axis, owing to the mentioned sign change). Panel (a) shows the section for  $\mu_3 = -0.09$  relative to the unit sphere for  $\mu_4 = 0.75$ ; panel (b) shows the corresponding bifurcation diagram in the  $(-\mu_1, \mu_2)$ -plane together with the paths for fold/subHopf and fold/homoclinic bursting; and panel (c) is an enlargement to highlight the transition to fold/homoclinic bursting. An important observation in Fig. 4(b) is the presence of two codimension-two Bogdanov–Takens points, denoted  $\text{BT}_r$  and  $\text{BT}_r^{\text{far}}$ , on the saddle-node bifurcation curve  $\text{SN}_r$ . The point  $\text{BT}_r^{\text{far}}$  has the same local unfolding as  $\text{BT}_r$  in Fig. 3, but the Hopf bifurcation in the local unfolding of  $\text{BT}_r$  in Fig. 4(b) is supercritical. This implies that the bifurcation diagram on a sphere of sufficiently small radius  $R \ll 1$  in Fig. 4(a) is, in fact, topologically that near the degenerate Bogdanov–Takens singularity of focus type, that is, case (M) of Fig. 1.

### 3 Transitions of bifurcation diagram on a sphere

The analysis in [15] started with the hypothesis that there exist a bifurcation diagram on the unit sphere for a suitable choice of  $\mu_4$  in system (1) such that both fold/subHopf and fold/homoclinic bursting could be generated by paths on this

sphere. As we argued above, this is not actually the case. Moreover, these initial investigations indicated that the transition from case (A) to case (M) does exist, but that the sequence of codimension-three bifurcations on a sphere in  $(\mu_1, \mu_2, \mu_3)$ -space is not exactly as proposed in [12] and shown in Fig. 1. In particular, it seems that there is no cusp point on the curve D of double limit cycles that disappears in a codimension-three singularity on  $L_b$  in between case (L) and case (M) in Fig. 1.

As was mentioned at the end of Sec. 2, the bifurcation diagram on the sphere changes topologically when its radius is decreased. We now consider this aspect of the codimension-four unfolding in more detail. As was already known from [12], for sufficiently large  $\mu_4$  the bifurcation diagram on a sphere with a fixed radius is that of the nilpotent focus of codimension three as presented in [6]. Here sufficiently large  $\mu_4$  means sufficiently large *relative to*  $\mu_1, \mu_2$  and  $\mu_3$ . Hence, for any given value of  $\mu_4 > 0$  this is satisfied on any sphere with sufficiently small radius  $R = \sqrt{\mu_1^2 + \mu_2^2 + \mu_3^2}$ , which has the following interesting consequence. Suppose one considers a sphere of a given fixed radius, say, with  $R = 1$ , with the bifurcation diagram of case (A) in Fig. 1 on it. As soon as  $\mu_4 > 0$  then bifurcation diagram (M) of the nilpotent focus of codimension three can already be found inside this given sphere on a sufficiently small sphere close to the central singularity! This observation means, in particular, that one finds the entire transition of bifurcation diagrams from case (A) to case (M) on nested spheres when one reduces the radius  $R$  down to zero.

Of course, it is also natural to keep the radius of the chosen sphere of interest constant, say, again at  $R = 1$ . As  $\mu_4$  is increased from 0, case (M) can be found on larger and larger spheres until it can be found on the chosen sphere. Hence, the entire transition is ‘pushed through’ the chosen sphere. In other words, increasing  $\mu_4$  while considering a sphere of a given radius is equivalent in this sense with decreasing the radius of the sphere considered while keeping  $\mu_4 > 0$  constant.

Another consequence of this observation is the following. For  $\mu_4 = 0$  the bifurcation diagram in  $(\mu_1, \mu_2, \mu_3)$ -space has cone structure, so is topologically the same on any sphere. For  $\mu_4 > 0$  it also has cone structure, but only in a small neighborhood of the origin, meaning that one finds case (M) of Fig. 1, the unfolding of the nilpotent focus of codimension three, on any sufficiently small sphere. Any of the other bifurcation diagrams (B) to (L) in Fig. 1, on the other hand, do not correspond to bifurcation diagrams in  $(\mu_1, \mu_2, \mu_3)$ -space that have cone structure. In particular, this means that the exact sequence of transitions one finds from case (A) to case (M) depends on the properties of the family of closed convex surfaces around the origin (such as spheres, ellipses or parallelepipeds).

Since it is arguably the most natural choice, we consider in what follows the bifurcation diagram on a sphere in  $(\mu_1, \mu_2, \mu_3)$ -space, where we concentrate on the transition from about case (G) to case (M) in system (1); this corresponds to the transition from the sphere in Figs. 3, where fold/subHopf bursting was found, to the limiting case of the degenerate Bogdanov–Takens singularity of focus type.

We first present in Fig. 5 topological sketches of this transition, as observed numerically via the computation of bifurcation diagrams on spheres that will be presented next. In the topological sketches in Fig. 5 the projections are reflected with respect to the vertical axis when compared with Fig. 1; in other words, the view is from outside the sphere, so that the projections better resemble the bifurcation diagrams on the sphere shown in Figs. 3 and 4, and in similar figures below. The starting point in Fig. 5 is case (G’), which is as the bifurcation diagram in Fig. 3(a). Case (G’) lies ‘in between’ cases (G) and (H) in Fig. 1 as far as the position of

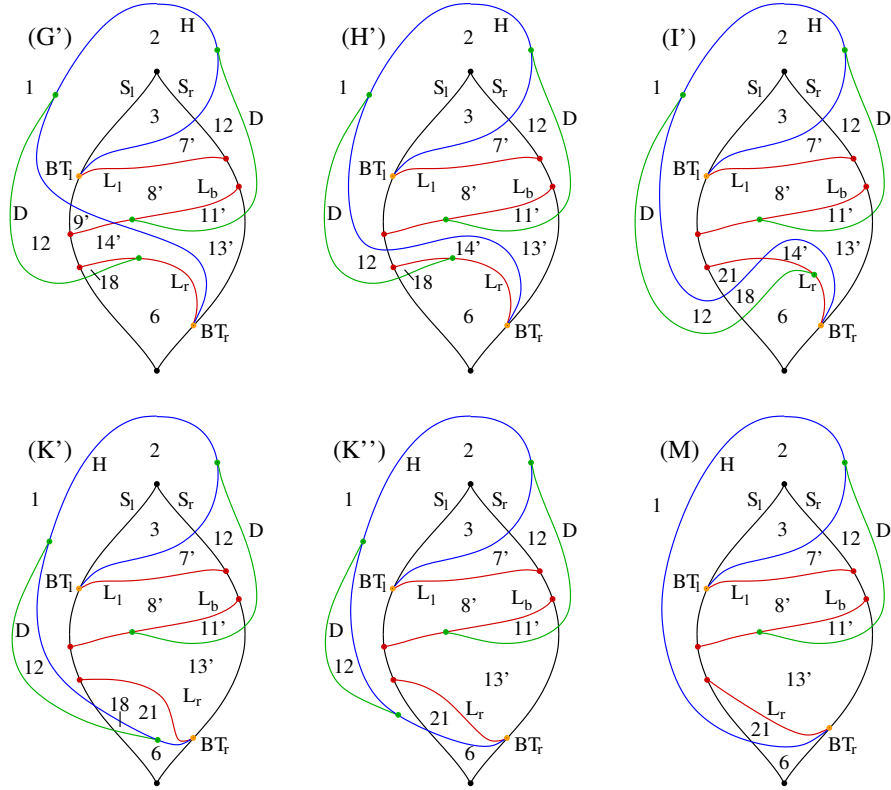


**Fig. 5.** Transition for increasing  $\mu_4$  as found numerically for system (1); shown are projections of unfoldings on a sphere in  $(\mu_1, \mu_2, \mu_3)$ -space for fixed  $\mu_4$ .

the Hopf curve  $H$  is concerned, but notice the absence of a cusp point on curve  $D$ . The curve  $H$  then crosses the end points of the curves  $L_b$  and  $L_r$  on  $S_l$ , yielding cases  $(H')$  and  $(I')$  of Fig. 5, respectively. Subsequently, there is a sign-change in the higher-order terms of the Bogdanov–Takens bifurcation  $BT_r$  to give case  $(K')$ , where the relative position of the curves  $H$  changes locally near  $BT_r$ . An important aspect is that there are now three degenerate Hopf bifurcation points on the curve  $H$ . The one inside the area bounded by  $S_l$  and  $S_r$  then moves through  $S_l$  to give case  $(K'')$ . The associated curve  $D$  of double periodic orbits then disappears when the respective two degenerate Hopf points that bound it come together and disappear; this codimension-three doubly degenerate Hopf point does not seem to involve additional bifurcations, but its further analysis is beyond the scope of this contribution. The final result is case  $(M)$ , the bifurcation diagram of the degenerate Bogdanov–Takens singularity of focus type.

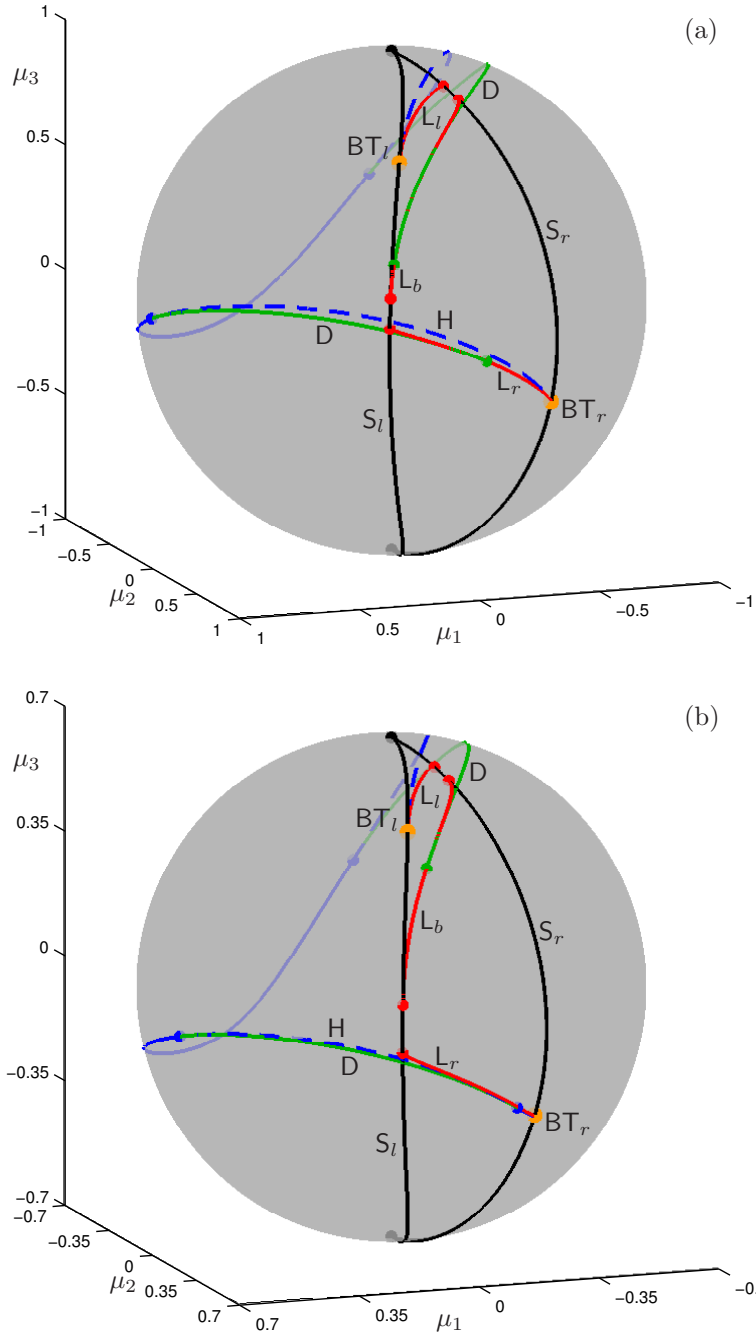


**Fig. 6.** Bifurcation diagrams of system (1) for  $\mu_4 = 1$  on a sphere of radius  $R$  in  $(\mu_1, \mu_2, \mu_3)$ -space; from (a) to (d),  $R = 1, R = 0.7, R = 0.5$  and  $R = 0.2$ .

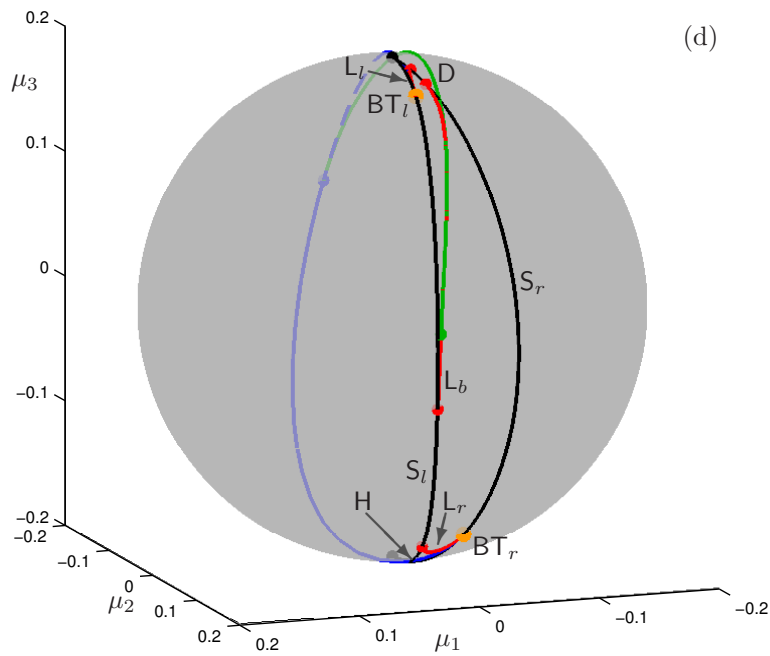
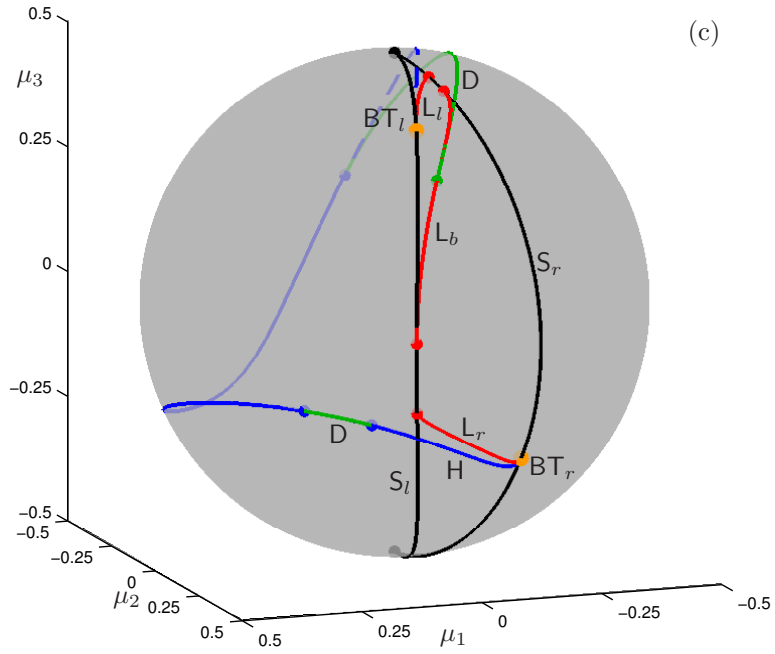
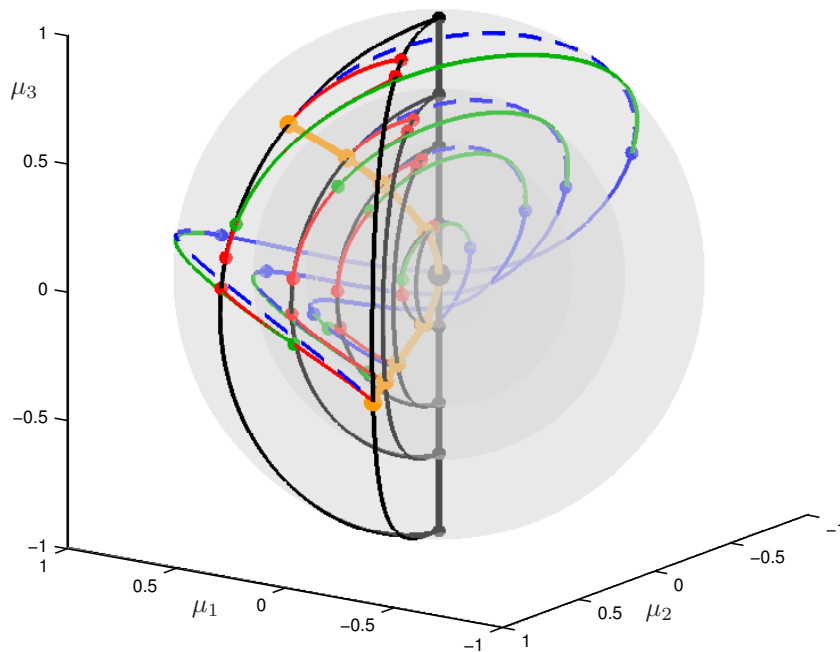


Fig. 6. continued



**Fig. 7.** The bifurcation diagrams of system (1) for  $\mu_4 = 1$  on the nested spheres in  $(\mu_1, \mu_2, \mu_3)$ -space of radius  $R = 1, R = 0.7, R = 0.5$  and  $R = 0.2$ .

Figure 6 presents numerical evidence of the transition as images of computed bifurcation diagrams of system (1) for  $\mu_4 = 1$  on spheres of radius  $R = 1, R = 0.7, R = 0.5$  and  $R = 0.2$ ; these computations were performed with the packages MATCONT [4] and AUTO [5]. The bifurcation diagram in Fig. 6(a) for  $R = 1$  is as case (H') in Fig. 5. Figure 6(b) shows the bifurcation diagram on the sphere of radius  $R = 0.7$ , where the Hopf curve H has dipped below the end point of  $L_r$  on  $S_l$ , as is sketched in case (I') of Fig. 5. Figure 6(c) for  $R = 0.5$  is past the type change of the Bogdanov–Takens point  $BT_r$ ; moreover, the associated curve D is already quite short and lies entirely outside the region bounded by  $S_l$ , and  $S_r$ , as in case (K'') of Fig. 5. Finally, for  $R = 0.2$ , as shown in Figure 6(d), we find case (M).

For illustration purposes, each sphere in Fig. 6 was rendered at the same size, irrespective of its actual radius. Figure 7, on the other hand, shows how the respective bifurcation diagrams are nested by rendering all spheres in  $(\mu_1, \mu_2, \mu_3)$ -space in one and the same image. Also shown is the vertical line of cusp bifurcations and the curve of Bogdanov–Takens bifurcations, which meet in a tangency at the origin, that is, at the nilpotent focus of codimension three (since  $\mu_4 = 1 > 0$ ). Taken together, Fig. 6 and Fig. 7 constitute numerical evidence in support of the revised transition presented in Fig. 5.

## 4 Conclusions

Unfoldings of codimension-four singularities of vector fields are sometimes seen as quite esoteric. The conjectural unfolding of codimension four that was originally presented in 1998 was almost a bit of an afterthought of the paper in [12], which deals with a codimension-three singularity that gives rise to symmetric bifurcation diagrams in planar sections nearby that had been found in numerous applications. Quite a number of years later it provided the solution, found 2012 in [15], to the question of where pseudo-plateau or fold/subHopf bursting can be found and whether and how it is connected to fold/homoclinic bursting.

The important aspect here is that the conjectural unfolding was presented in [12] as a sequence of bifurcation diagrams on spheres that constitutes the transition from the codimension-three unfolding considered in [12] to the well-known degenerate Bogdanov–Takens bifurcation of focus type that was known from [6]. As a result of the renewed interest in this transition we realized that the transition is, in some sense, not so well defined. More specifically, the bifurcation diagrams found in the transition on convex surfaces (such as spheres or ellipses) are not uniquely defined due to the lack of cone structure. On the other hand, it is quite natural to consider spheres in parameter space, in which case an amended sequence of transitions can be determined with the help of numerical continuation tools. Overall, the different bifurcation diagrams can be encountered on nested spheres as soon as  $\mu_4 > 0$  in (1), rather like Russian dolls. As  $\mu_4$  is increased they emerge one-by-one on a chosen fixed sphere, such as the unit sphere in  $(\mu_1, \mu_2, \mu_3)$ -space.

We presented here only the part of the codimension-four unfolding that is relevant for generating the different types of bursting action potentials considered in [15]. Indeed, the complete transition between the codimension-three singularity for  $\mu_4 = 0$  and the degenerate Bogdanov–Takens bifurcation of focus type can be represented in the same spirit in terms of bifurcation diagrams on nested spheres for  $\mu_4 = 1$ . The overall sequence of bifurcation diagrams, to be presented elsewhere, will shed light on the manifestation of the relevant bifurcations known from [12] and the study [3] of an alternative parameterization.

## Acknowledgments

The work presented here is quite directly related to work of and with Christiane Rousseau, and it is a pleasure to have this opportunity to thank her for explicit and implicit support and encouragement during many years. She was instrumental in getting us into unfoldings on spheres and compactifications of phase spaces, techniques that we keep using throughout our work. We have been enjoying meeting Christiane in many different places, including regularly during our visits to Montréal of course. We also thank our co-authors Alexander Khibnik, Arthur Sherman and Krasimira Tsaneva-Atanasova, who have been great companions in this unfolding adventure.

## References

1. A. D. Bazykin, Yu. A. Kuznetsov and A.I. Khibnik, Bifurcation diagrams of planar dynamical systems, *Research Computing Center, Pushchino*, Preprint, 1985 (in Russian).
2. R. Bertram, M. J. Butte, T. Kiemel, and A. Sherman, Topological and phenomenological classification of bursting oscillations, *Bulletin of Mathematical Biology* **57**(3):413–439, 1995.
3. G. Dangelmayr and J. Guckenheimer, On a four parameter family of planar vector fields, *Archive Rational Mechanics* **97**:321–352, 1987.
4. A. Dhooge, W. Govaerts, and Yu. A. Kuznetsov. MATCONT: A MATLAB package for numerical bifurcation analysis of ODEs. *ACM Transactions of Mathematics Software* **29**(2):141–164, 2003; available via <http://www.matcont.ugent.be/>.
5. E. J. Doedel, AUTO: Continuation and bifurcation software for ordinary differential equations, with major contributions from A. R. Champneys, T. F. Fairgrieve, Yu. A. Kuznetsov, B. E. Oldeman, R. C. Paffenroth, B. Sandstede, X. J. Wang and C. Zhang, 2007; available via <http://cmvl.cs.concordia.ca/>.
6. F. Dumortier, R. Roussarie and J. Sotomayor, Generic 3-parameters families of planar vector fields, unfoldings of saddle, focus and elliptic singularities with nilpotent linear parts, in F. Dumortier, R. Roussarie, J. Sotomayor and H. Zoladek (eds.), *Bifurcations of Planar Vector Fields: Nilpotent Singularities and Abelian Integrals*, Lecture Notes in Mathematics Vol. **1480**, Springer-Verlag, Berlin, 1991, pp. 1–164.
7. M. Golubitsky, K. Josić and T. J. Kaper, An unfolding theory approach to bursting in fast-slow systems, in H. W. Broer, B. Krauskopf, and G. Vegter (eds.), *Global Analysis of Dynamical Systems*, Institute of Physics Publishing, Bristol, 2001, pp. 277–308.
8. F. van Goor, Y. Li, and S. Stojilkovic, Paradoxical role of large-conductance calcium-activated  $K^+$  BK channels in controlling action potential-driven  $Ca^{2+}$  entry in anterior pituitary cells, *J. Neurosci.* **21**(16):5902–5915, 2001.
9. J. Guckenheimer and S. Malo, Computer-generated proofs of phase portraits for planar systems, *Int. J. Bifurcation Chaos* **6**(5):889–892, 1996.
10. A. L. Hodgkin and A. F. Huxley, A quantitative description of membrane current and its application to conduction and excitation in nerve, *The Journal of Physiology* **117**(4):500–544, 1952.
11. F. C. Hoppensteadt and E. M. Izhikevich, *Weakly Connected Neural Networks*, Springer-Verlag, New York, 1997.
12. A. I. Khibnik, B. Krauskopf, and C. Rousseau, Global study of a family of cubic Liénard equations, *Nonlinearity* **11**(6):1505–1519, 1998.
13. A. P. LeBeau, A. B. Robson, A. E. McKinnon, and J. Sneyd, Analysis of a reduced model of corticotroph action potentials, *J. Theor. Biol.* **192**(3):319–339, 1998.
14. S. Malo, Rigorous computer verification of planar vector field structure, *Ph.D.-thesis, Cornell University*, 1994.
15. H. M. Osinga, A. Sherman and K. T. Tsaneva-Atanasova, Cross-currents between biology and mathematics: The codimension of pseudo-plateau bursting, *Discrete and Continuous Dynamical Systems—Series A* **32**(8):2853–2877, 2012.
16. B. van der Pol, A theory of the amplitude of free and forced triode vibrations, *Radio Review* **1**:701–710, 1920.

17. B. van der Pol, On relaxation oscillations, *The London, Edinburgh and Dublin Philosophical Magazine Series 7* **2**:978–992, 1926.
18. J. Rinzel, Bursting oscillations in an excitable membrane model, in B. D. Sleeman and R. D. Jarvis (eds.), *Ordinary and Partial Differential Equations*, Lecture Notes in Mathematics Vol. **1151**, Springer-Verlag, New York, 1985, pp. 304–316.
19. J. Rinzel, A formal classification of bursting mechanisms in excitable systems, in A. M. Gleason (ed.), *Proceedings of the International Congress of Mathematicians* Vol 1, 2, American Mathematical Society, Providence RI, 1987, pp. 1578–1593; also (with slight differences) in E. Teramoto and M. Yamaguti (eds.), *Mathematical Topics in Population Biology, Morphogenesis and Neuroscience*, Lecture Notes in Biomathematics Vol. **71**, Springer-Verlag, Berlin, 1987, pp. 267–281.
20. J. V. Stern, H. M. Osinga, A. LeBeau, and A. Sherman, Resetting behavior in a model of bursting in secretory pituitary cells: Distinguishing plateaus from pseudo-plateaus, *Bulletin of Mathematical Biology* **70**(1):68–88, 2008.
21. K. Tsaneva-Atanasova, A. Sherman, F. van Goor, and S. Stojilkovic, Mechanism of spontaneous and receptor-controlled electrical activity in pituitary somatotrophs: experiments and theory, *J. Neurophysiol.* **98**(1):131–144, 2007.
22. X. Wang and R. E. Kooij, Limit cycles in a cubic system with a cusp, *SIAM J. Math. Anal.* **23**(6):1609–1622, 1992.